Clinical Neurophysiology xxx (2012) xxx–xxx

Contents lists available at SciVerse ScienceDirect

Clinical Neurophysiology

journal homepage: www.elsevier.com/locate/clinph

Automated single-trial assessment of laser-evoked potentials as an objective functional diagnostic tool for the nociceptive system

S.M. Hatem [a,b,c], L. Hu [d,e], M. Ragé [a], A. Gierasimowicz [c], L. Plaghki [a], D. Bouhassira [b,f], N. Attal [b,f], G.D. Iannetti [d], A. Mouraux [a,*]

[a] Institute of Neuroscience (IONS), Université catholique de Louvain, Brussels, Belgium
[b] INSERM U-987, Pathophysiology and Clinical Pharmacology of Pain, CHU Ambroise Paré, Boulogne-Billancourt, France
[c] Clinique de Médecine Physique et Réadaptation, CHU Brugmann, Brussels, Belgium
[d] Department of Neuroscience, Physiology and Pharmacology, University College London, London, United Kingdom
[e] Key Laboratory of Cognition and Personality (Ministry of Education) and School of Psychology, Southwest University, Chongqing, China
[f] Versailles Saint-Quentin University, Versailles, France

ARTICLE INFO

Article history:
Accepted 15 May 2012
Available online xxxx

Keywords:
Laser-evoked potentials (LEPs)
Single-trial analysis
Wavelet denoising
Multiple linear regression
Event-related potentials (ERPs)
Syringomyelia
Neuropathic pain

HIGHLIGHTS

- This study demonstrates the clinical usefulness of an automated analysis of ERPs to assess nociceptive pathways.
- For clinical research, the automated approach provides an unbiased solution to characterize ERPs, even when difficult to identify by visual inspection.
- For evidence-based medicine, the automated approach overcomes the important problem related to the subjectivity of a visual interpretation of ERPs.

ABSTRACT

Objective: To assess the clinical usefulness of an automated analysis of event-related potentials (ERPs).
Methods: Nociceptive laser-evoked potentials (LEPs) and non-nociceptive somatosensory electrically-evoked potentials (SEPs) were recorded in 37 patients with syringomyelia and 21 controls. LEP and SEP peak amplitudes and latencies were estimated using a single-trial automated approach based on time-frequency wavelet filtering and multiple linear regression, as well as a conventional approach based on visual inspection.
Results: The amplitudes and latencies of normal and abnormal LEP and SEP peaks were identified reliably using both approaches, with similar sensitivity and specificity. Because the automated approach provided an unbiased solution to account for average waveforms where no ERP could be identified visually, it revealed significant differences between patients and controls that were not revealed using the visual approach.
Conclusion: The automated analysis of ERPs characterized reliably and objectively LEP and SEP waveforms in patients.
Significance: The automated single-trial analysis can be used to characterize normal and abnormal ERPs with a similar sensitivity and specificity as visual inspection. While this does not justify its use in a routine clinical setting, the technique could be useful to avoid observer-dependent biases in clinical research.

1. Introduction

Studying the neural activity related to the activation of nociceptors and the conduction of nociceptive input within somatosensory pathways constitutes a real challenge in the sense that only few external stimuli have the ability to activate nociceptors selectively. Pulses of radiant-heat, such as those which can be delivered by infrared laser stimulators, allow activating nociceptive afferents selectively (Plaghki and Mouraux, 2003). The recording of event-related brain potentials (ERPs) in response to brief laser stimuli has been described in numerous studies (Garcia-Larrea et al., 2003) and, at present, laser-evoked potentials (LEPs) are regarded as the best available method to explore the nociceptive system in

* Corresponding author. Address: Institute of Neuroscience, Université catholique de Louvain, 53 Avenue Mounier, 1200 Brussels, Belgium. Tel.: +32 764 93 49; fax: +32 764 53 60.
E-mail address: andre.mouraux@uclouvain.be (A. Mouraux).

1388-2457/$36.00
http://dx.doi.org/10.1016/j.clinph.2012.05.007

humans in a large variety of clinical conditions (Cruccu et al., 2010; Haanpaa, 2011; Haanpaa et al., 2011; Treede et al., 1991, 2003; Casanova-Molla et al., 2011; Orstavik et al., 2006; Quante et al., 2007; Hatem et al., 2009, 2010; Kakigi et al., 1991, 1992; Casey et al., 1996; Garcia-Larrea et al., 2002; Spiegel et al., 2003).

Until now, visual inspection of ERP waveforms has been regarded as the generally agreed-on method to identify the different waves of ERPs. The different ERP waves can be characterized based on their latency relative to stimulus onset, their polarity, their amplitude and/or their scalp topography, which can then be compared to that of normative data (Luck, 2005). The assessment of a LEP response is usually determined according to the following criteria. The bulk of the LEP waveform at Cz should consist of (1) a positive deflection preceded by a negative deflection, (2) appearing within a defined time-interval (e.g. <500 ms when stimulating the hand), and (3) displaying a scalp topography with a maximum at the vertex (Carmon et al., 1976).

However, there are several important limitations underlying the identification of ERPs using visual inspection for its use in clinical research. First, and most important, the identification of the different components of the recorded ERP waveform is necessarily dependent of the observer (Kramer, 1985). Hence, in the context of clinical studies, it is mandatory that their identification and characterization be performed in a blinded fashion – and even so, there is an unavoidable bias related to the subjective judgment of the observer. Second, the identification and characterization of ERPs becomes equivocal when one or more criteria used to define the normality of the ERP waveforms are not fulfilled. Third, an important question arises as to how to consider ERP waveforms in which no peak can be recognized visually. Discarding those ERP waveforms inevitably biases group-level results towards an underestimation of the pathological or experimentally-induced reduction in ERP magnitude. Conversely, arbitrarily assigning a null magnitude to the ERP amplitude inevitably biases group-level results towards overestimation (Hu et al., 2010; Mayhew et al., 2006). Furthermore, no information concerning the latency of the elicited responses can be extracted from these waveforms which, therefore, cannot be included in group-level comparisons. For all these reasons, an observer-independent technique to estimate the magnitude and latency of ERPs is highly desirable (Moher et al., 2010).

Recently, Mayhew et al. (2006) and Hu et al. (2010) developed an automated, observer-independent method to estimate reliably the N1, N2 and P2 peaks of LEPs in healthy controls. Their most current approach is based on a combination of methods to enhance the signal-to-noise ratio of ERPs using a time-frequency filter based on the wavelet transform, and a multiple linear regression analysis to estimate peak amplitudes and latencies at the level of single trials. In their seminal study, it was shown that this approach is effective at estimating the latency and amplitude of ERPs recorded in young, healthy volunteers. However it remains to be demonstrated whether the automated approach can be used in patients exhibiting ERP waveforms that are intrinsically difficult to recognize (because of abnormal amplitudes, latencies and morphology). Hence, prior to implementing the automated approach in the context of clinical research, it is fundamental to assess its ability to recognize pathological ERP waveforms in patients with a good sensitivity and specificity.

The aim of the present study was thus to assess the *clinical* usefulness of this novel automated approach (Mouraux and Guerit, 2011) by examining its sensitivity and specificity to detect abnormal LEPs recorded in patients with syringomyelia vs. healthy controls. Indeed, patients with symptomatic syringomyelia often exhibit abnormal LEPs due to a selective thermoalgesic sensory deficit resulting from the compression of the anterior commissure of the spinal cord by the liquid-filled central cavity, which thus affects spinothalamic pathway function. The same automated approach was also applied to the analysis of late-latency SEPs, thereby assessing the lemniscal pathway which is most-often preserved in syringomyelia (Kakigi et al., 1991; Treede et al., 1991; Bromm and Treede, 1991). The estimates of LEPs and SEPs obtained using this automated approach were quantitatively and directly compared with the estimates obtained using conventional visual inspection of ERP waveforms.

2. Methods

2.1. Subjects

Data was collected in 37 syringomyelia patients (46 ± 13 years; 25 women) and 21 sex- and age-matched healthy controls (45 ± 15 years; 13 women). The patients were recruited in the pain clinics and in the departments of neurosurgery and orthopaedics of the Ambroise Paré Hospital (Boulogne-Billancourt, France), the Kremlin-Bicêtre University Hospital (Bicêtre, France) and the Cliniques universitaires St-Luc (Brussels, Belgium). All patients had a MRI-diagnosed, symptomatic syringomyelia, characterized by a clinical thermonociceptive deficit of the upper limbs (Hatem et al., 2010). Healthy volunteers had no clinical history, clinical symptoms or signs of peripheral or central nervous system disorders, and no abnormalities on MR images of the cervical spinal cord. All participants gave written informed consent, and the local ethics committees approved the procedures.

2.2. Nociceptive laser stimulus

LEPs were elicited by infrared CO_2 laser pulses (wavelength: 10.6 μm) applied to five different locations: left and right hand dorsum (dermatome C7), left and right shoulder (dermatome C4), and left hemiface (second division of the trigeminal nerve, V2). Stimulus duration was 50 ms and beam diameter at target site was 10 mm. Stimulus intensity was individually adjusted such that stimuli were perceived as clearly pricking in skin areas without sensory deficit. In patients, stimulus intensity was determined on the most affected hand, i.e. the hand presenting with the most severe sensory deficit. If patients could not perceive the thermal stimulus, the intensity was set arbitrarily to a level that was supraliminal for Aδ-nociceptors. In healthy controls, stimulus intensity was determined randomly on one of both hands and matched with the stimulus intensity of patients in order to avoid a bias due to different stimulation conditions. To avoid superficial burns (Plaghki and Mouraux, 2003), the maximum energy density was set to 11 mJ/mm^2. For each subject, the same energy density was then used at the five stimulus locations. Thirty trials, separated by a 5–10 s inter-stimulus interval, were recorded from each stimulation site.

2.3. Non-nociceptive electrical stimulus

Electrically-evoked SEPs were elicited by the transcutaneous electrical stimulation of the left and right *nervus radialis superficialis*. The electrical stimulus was produced by a constant current generator (Digitimer DS7, Digitimer Ltd., United Kingdom). Two electrodes (diameter: 10 mm; inter-electrode distance: 25 mm) were placed over the stimulated nerve, 5 cm proximal to the wrist of the hand. The electrical stimulus consisted of a square-wave pulse of 0.5 ms duration (Hatem et al., 2007). Stimulus intensity corresponded to twice the absolute detection threshold, avoiding any uncomfortable or unpleasant sensation. Thresholds were measured randomly on one of both hands and the same stimulus intensity was used for both hands. The stimulus produced a non-painful tingling sensation in the sensory territory of the *nervus radialis superficialis*. Twenty trials were recorded from each stimulation site.

Please cite this article in press as: Hatem SM et al. Automated single-trial assessment of laser-evoked potentials as an objective functional diagnostic tool for the nociceptive system. Clin Neurophysiol (2012), http://dx.doi.org/10.1016/j.clinph.2012.05.007

The order of stimulation sites and modalities (laser vs. electrical) was randomized across subjects.

2.4. Data acquisition

The EEG was recorded from 19 Ag–AgCl electrodes placed on the scalp according to the International 10–20 system. Linked earlobes (A1A2) were used as reference. Ground was placed at the wrist. Impedance was kept below 5 kΩ. Two electrodes, placed at the lower right and upper left corner of the right eye monitored ocular movements and eye blinks. Signals were amplified and digitized (gain: 1000; filter: 0.06–75 Hz, sampling rate: 167 Hz) using a PL-EEG recorder (Walter Graphtek, Germany).

2.5. Data pre-processing

Offline signal-processing steps were performed using BrainVision Analyzer 1.05 (Brain Products GmbH, Germany), the Letswave EEG toolbox (http://www.nocions.webnode.com/letswave) (Mouraux and Iannetti, 2008).

The EEG was segmented into 5000 ms long epochs ranging from −2000 to +3000 ms relative to stimulus onset, baseline-corrected (reference interval: −500 to 0 ms) and band-pass filtered (0.2 to 48 Hz). Electro-oculographic and electro-cardiographic artifacts were subtracted using a validated method based on an Independent Component Analysis (ICA) (Jung et al., 2000). In all datasets, Independent Components (ICs) related to ocular movements and eye blinks had a large electro-oculogram channel contribution and a frontal scalp distribution.

2.6. Data analysis

For each subject, average ERP waveforms were computed for each stimulus type and each stimulus location. In the control group, to assess the sensitivity and specificity of the visual and automated methods for identifying LEPs and SEPs, these average waveforms were further segmented into two distinct waveforms. The first waveform ranged from −0.5 to +1 s relative to stimulus onset (POSTSTIM), and was thus expected to contain the stimulus-evoked ERP. The second waveform ranged from −1.5 to 0 s relative to stimulus onset (PRESTIM), and was thus expected to only contain background EEG activity. In these epochs, the time-axis was shifted such that both PRESTIM and POSTSTIM average waveforms appeared to be segmented from −0.5 to +1 s relative to stimulus onset.

2.6.1. Visual identification of LEPs and SEPs

Two experimented blinded observers were asked to identify the peaks of LEPs and SEPs in each averaged waveform. Observers were informed of the stimulation site and stimulus modality. Average waveforms were presented in random order. Peak amplitudes were measured from baseline to peak.

Within each average LEP waveform three distinct peaks (LEP-N1, LEP-N2 and LEP-P2) were characterized as follows. After stimulation of the hand, the LEP-P2 was identified at electrode Cz as a positive component peaking between 300 and 500 ms after stimulus onset. The LEP-N2 was defined at electrode Cz as a negative peak preceding the LEP-P2 and occurring between 150 and 350 ms after stimulus onset. The LEP-N1 was searched for at the temporal electrode (T3 or T4) contralateral to the stimulus rereferenced to electrode Fz (Cruccu et al., 2008), and defined as the negative deflection preceding the LEP-N2 and occurring between 100 and 300 ms after stimulus onset. After stimulation of the shoulder and face, LEP peaks were recognized at shorter latencies than latencies of the hand, i.e. 20 ms shorter for the shoulder and 50 ms shorter for the face.

Within each average SEP waveform, two distinct peaks (SEP-N1, SEP-P2) were characterized as follows. After stimulation of the hand, the SEP-P2 was identified at electrode Cz as a positive component peaking between 150 and 300 ms after stimulus onset. The SEP-N1 was defined as a negative peak preceding the SEP-P2 at electrode Cz and occurring between 80 and 160 ms after stimulus onset.

2.6.2. Automated single trial analysis

The amplitude and latency of ERP components were estimated in each single trial of each subject, stimulus type and stimulation site using an automated single-trial analysis that consisted of two consecutive steps: wavelet filtering and multiple linear regression, using the N1-measure toolbox (http://www.iannettilab.webnode.com/n1measure) (Hu et al., 2010). The wavelet filter was used to enhance the signal-to-noise ratio (SNR) of ERPs. The multiple linear regression was used to obtain an automatic and unbiased estimation of the amplitude and latency of ERPs at the level of single trials.

2.6.2.1. Wavelet filtering. Wavelet filtering is a time-variant denoising method that can reduce the background noise and increase the SNR of the ERP responses significantly (Hu et al., 2010, 2011; Mouraux and Plaghki, 2004; QuianQuiroga and Garcia, 2003). First, single-trial ERPs were decomposed into a time-frequency representation using a continuous Morlet wavelet transform. For each stimulation site, an average time-frequency representation was constructed (group-level average). Based on their averaged time-frequency representation, specific areas on the time-frequency plane corresponding to the ERP responses were localized and used to generate a wavelet filtering template, as follows. Single-trial time-frequency matrixes were first averaged and then baseline-corrected by subtracting, for each estimated frequency, the average power of the signal enclosed in the time-interval ranging from −250 to 0 ms. Then, the average time-frequency matrixes were thresholded with the objective of keeping wavelet coefficients with high energy and eliminating wavelet coefficients with low energy. The empirical cumulative distribution function (CDF) of the normalized power spectrum was calculated by the Kaplan-Meier estimate (Lawless, 2003) and the filtering model was obtained by creating a matrix whose time-frequency pixels were set to 1 when the CDF of the corresponding wavelet coefficient was greater than the threshold, and set to 0 when the CDF of the corresponding wavelet coefficient was smaller than the threshold. The threshold was set to $0.85 * (\max(\mathrm{CDF}) - \min(\mathrm{CDF})) + \min(\mathrm{CDF})$, which allowed retaining the greater part of the ERP response while discarding as much noise as possible (see Hu et al., 2010 for details). Finally, time-domain ERP waveforms with a higher SNR were reconstructed using the inverse continuous wavelet transform.

2.6.2.2. Multiple linear regression. In order to estimate the amplitude and latency of ERP components in single trials in an unbiased fashion, a multiple linear regression method was applied to the wavelet filtered waveforms.

To model the N1 wave of LEPs, the multiple linear regression method was performed using the 0 to +300 ms post-stimulus time-interval. To model the N2 and P2 waves of LEPs, as well as the N1 and P2 waves of SEPs, the multiple linear regression method was performed using the 0–500 ms post-stimulus time-interval (note that when analyzing the resting EEG trials (PRESTIM), this actually corresponded to −1000 to −700 ms and −1000 to −500 ms before the onset of the stimulus respectively).

A single regressor and its temporal derivative were used to model the LEP-N1. These regressors were obtained from the across-trial group average waveform measured at the contralateral temporal electrode (T3 or T4) referenced to Fz, after wavelet filtering. Two regressors and their temporal derivatives were used to

Please cite this article in press as: Hatem SM et al. Automated single-trial assessment of laser-evoked potentials as an objective functional diagnostic tool for the nociceptive system. Clin Neurophysiol (2012), http://dx.doi.org/10.1016/j.clinph.2012.05.007

model the LEP-N2 and LEP-P2, as well as the SEP-N1 and SEP-P2. These regressors were obtained from the across-trial group average waveform measured at the electrode Cz referenced to A1A2, after wavelet filtering. The inclusion of temporal derivatives allowed modeling the temporal variability of the response, thus yielding an estimate of both the amplitude and latency of each modeled ERP wave. These basis sets were then regressed against each single EEG epoch.

Using the fitted waveforms, the amplitude and latency of the ERP responses in each single trial were measured by finding: (1) for the LEP-N1 and LEP-N2 as well as for the SEP-N1, the most negative peak for a positive fit or the most positive peak for a negative fit, within a 100-ms wide time window centered on the latency of the corresponding ERP peak identified in the average waveform; (2) for the LEP-P2 and SEP-P2, the most positive peak for a positive fit or the most negative peak for a negative fit, within a 100-ms wide time window centered on the latency of the corresponding ERP peak in the average waveform. Finally, for each subject and stimulation site, single-trial amplitudes and latencies were averaged across trials.

2.7. Statistical analysis

2.7.1. Inter-rater reliability of the visual inspection of ERPs

The inter-rater reliability of the conventional identification of ERPs using visual inspection performed by each of the two independent observers was assessed by calculating the absolute agreement between two observers using two-way mixed intra-class correlation coefficients (single measure). Paired *t*-tests were used to assess differences of ERP peak measurements between the two observers.

2.7.2. Sensitivity and specificity

To assess the sensitivity and specificity of the automated approach and compare it to the sensitivity and specificity of the conventional approach, receiver operating characteristic (ROC) curves were constructed using the peak-to-peak ERP amplitudes estimated using each of the two approaches. The average waveforms obtained using the EEG epochs with no ERP (i.e. epochs segmented from −1.5 to 0 s relative to stimulus onset, PRESTIM) as well as the average waveforms obtained using the EEG epochs expected to contain an ERP (i.e. epochs segmented from −0.5 to 1 s relative to stimulus onset, POSTSTIM) of healthy controls entered this analysis. The ROC curves were used to determine the sensitivity and specificity of the two approaches as a function of ERP amplitude cut-off value, as well as to determine the amplitude cut-off value that was associated with the lowest rate of false-negatives, i.e. the highest sensitivity to recognize the absence of an ERP.

2.7.3. Performance at detecting LEP and SEP abnormalities

A one-way analysis of variance (ANOVA) was used to compare both approaches with respect to the amplitudes and latencies of the ERP peaks obtained at each stimulation site in the patients and the healthy controls. When no ERP components could be recognized visually, amplitudes and latencies were regarded as missing values. Furthermore, the inter-rater agreement between the two approaches was assessed using two-way mixed intra-class correlation coefficients (absolute agreement) and paired *t*-tests.

Results were expressed as mean ± 1 SD, except if otherwise specified. In all cases, $p < 0.05$ was considered significant.

3. Results

In total, 392 average ERP waveforms were recorded: 290 LEP waveforms and 102 SEP waveforms. The mean energy density used for laser stimulation was 9.5 ± 2.7 mJ/mm^2 in patients and 9.3 ± 0.8 mJ/mm^2 in controls. The mean intensity of electrical stimulation was 1.4 ± 0.5 mA in patients and 1.2 ± 0.1 mA in controls. These stimulus parameters were not significantly different between groups. The grand-average waveforms obtained after stimulation of each body site are shown in Fig. 1. A more detailed description of the clinical and electrophysiological findings of the syringomyelia patients included in the present study can be found in Hatem et al. (2010).

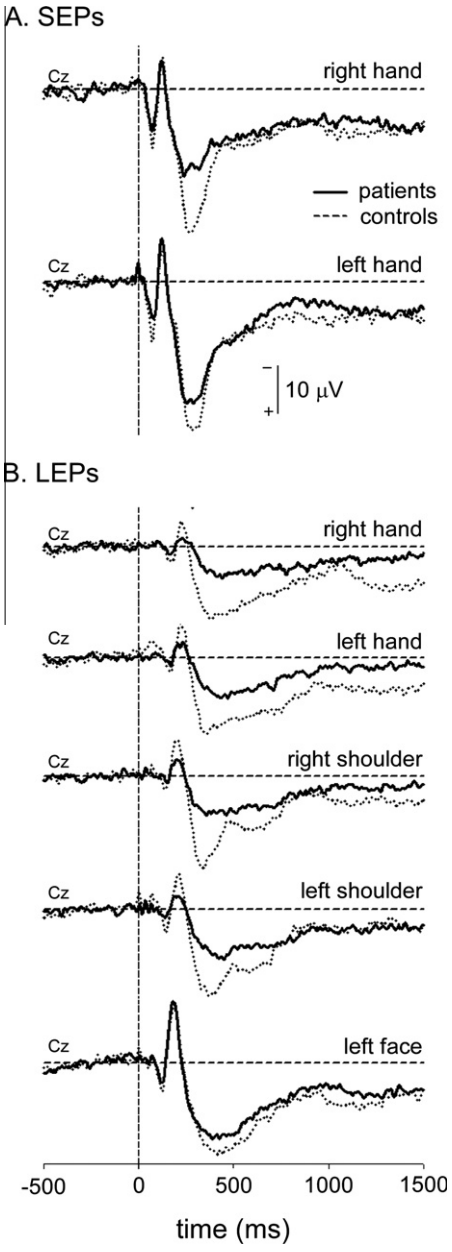

Fig. 1. Grand-average waveforms of nociceptive laser-evoked potentials (LEPs) and non-nociceptive somatosensory electrically-evoked potentials (SEPs) recorded in patients (bold) and healthy controls (dotted) (electrode Cz vs. A1A2).

3.1. Inter-rater reliability of the visual inspection of ERPs

The inter-rater agreement between the two blinded observers was excellent for both LEP and SEP waveforms, especially for amplitude measurements (intra-class correlation coefficients: 0.99–1). Accordingly, paired *t*-tests showed no significant differ-

Please cite this article in press as: Hatem SM et al. Automated single-trial assessment of laser-evoked potentials as an objective functional diagnostic tool for the nociceptive system. Clin Neurophysiol (2012), http://dx.doi.org/10.1016/j.clinph.2012.05.007

ences between the visual measurements performed by the two observers, except for LEP-P2 latencies which were regarded shorter by one of the observers. This difference may be due to the occasional ambiguity between the LEP-P2 peak and an additional later positive peak occurring in some subjects (Legrain et al., 2005; Siedenberg and Treede, 1996). Due to the overall excellent agreement between the two observers, comparison of the results obtained using the automated approach was compared to the results of a single observer (SH).

3.2. Sensitivity and specificity of automated and visual ERP identification in healthy controls

Values of peak-to-peak amplitudes obtained in healthy controls using the visual and automated approaches are shown in Fig. 2 (LEP: N2-P2; SEP: N1-P2). For each method (visual identification and automated identification), a receiver-operating characteristic (ROC) curve of peak-to-peak amplitude was constructed, using the type of epoch (PRESTIM vs. POSTSTIM) as state variable. Areas under the ROC curve were not significantly different between the visual analysis (0.93 ± 0.019 (SEM) for LEPs and 0.97 ± 0.016 for SEPs) and the automated analysis, (0.93 ± 0.021 for LEPs and 1.00 ± 0.0 for SEPs). For each identification method, the cut-off amplitude value which provided an optimal sensitivity and specificity was calculated from the ROC. This cut-off value corresponded to the peak-to-peak amplitude that optimally distinguished between PRESTIM vs. POSTSTIM waveforms.

For the approach based on visual inspection, the optimal cut-off value for detecting LEPs in our sample of subjects was 12.5 μV, resulting in a sensitivity of 91% and a specificity of 86%. The optimal cut-off value for detecting SEPs was 18.9 μV, resulting in a sensitivity of 95% and a specificity of 90%.

For the approach based on the automated single-trial estimation of ERPs, the optimal cut-off value for detecting LEPs was 9.3 μV, resulting in a sensitivity of 99% and a specificity of 84%. The optimal cut-off value for detecting SEPs was 9.3 μV, resulting in sensitivity of 100% and a specificity of 100%.

The observer-dependent sensitivity and specificity for visually classifying PRESTIM and POSTSTIM waveforms was also calculated. For this purpose, the blinded observers were asked to categorize each waveform as containing or lacking an ERP according to the visual identification criteria described in the Introduction. The observer-dependent visual identification method had a slightly lower sensitivity and specificity (LEP: sensitivity 96% – specificity 83%; SEP: sensitivity: 95% – specificity 95%) than the automated approach.

3.3. Performance of visual and automated ERP identification at detecting LEP and SEP abnormalities in patients

The estimation of LEP and SEP amplitudes and latencies using the approach based on visual inspection is reported in Table 1. Using this approach, no ERP could be identified in 49 (12.5%) average waveforms, which were thus considered as missing values in the analyses (Table 2). All of these waveforms corresponded to LEPs recorded in patients. All LEP and SEP waveforms in healthy controls were correctly recognized by visual inspection. No significant differences of amplitudes were observed between patients and controls, except for the latency of the LEP-N1 component, which was delayed in patients vs. healthy controls.

The estimation of LEP and SEP amplitudes and latencies using the automated approach is reported in Table 3. Using this approach, LEP amplitudes (LEP-N1 amplitude, LEP N2-P2 peak-to-peak amplitude) elicited by stimulation of the hands and shoulders were significantly reduced in patients vs. controls.

Comparison of the estimates obtained using the visual and automated approaches showed that the absolute agreement between the two approaches was high, especially when considering the estimation of ERP amplitude (Fig. 3). Paired *t*-tests showed that peak-to-peak amplitudes of LEPs and SEPs estimated using the automated approach were slightly smaller than peak-to-peak amplitudes of LEPs and SEPs estimated using the visual approach. Similarly, the latencies of LEP and SEP peaks estimated using the visual approach were slightly delayed as compared to the latencies of LEP and SEP peaks estimated using the automated approach (Table 4).

As stated above, using the approach based on visual inspection, no LEP could be identified in 49 ERP waveforms. Importantly, the peak amplitudes obtained by applying the automated approach to these LEP waveforms were, on average, significantly different from zero (LEP-N1: −1 ± 2 μV, $p = 0.040$; LEP-N2: −2 ± 4 μV, $p < 0.001$; LEP-P2: 2 ± 3 μV, $p < 0.001$; mean ± SD; *t*-test) (see also Fig. 3). This indicates that, at least in a fraction of trials, the laser stimulus *did* elicit an LEP, even though it could not be identified visually in the average LEP waveform. To ensure that this finding did not result from a bias in the automated approach, we also calculated the average estimated amplitude of LEPs in the PRESTIM trials, i.e. in which no ERP was present. These estimated

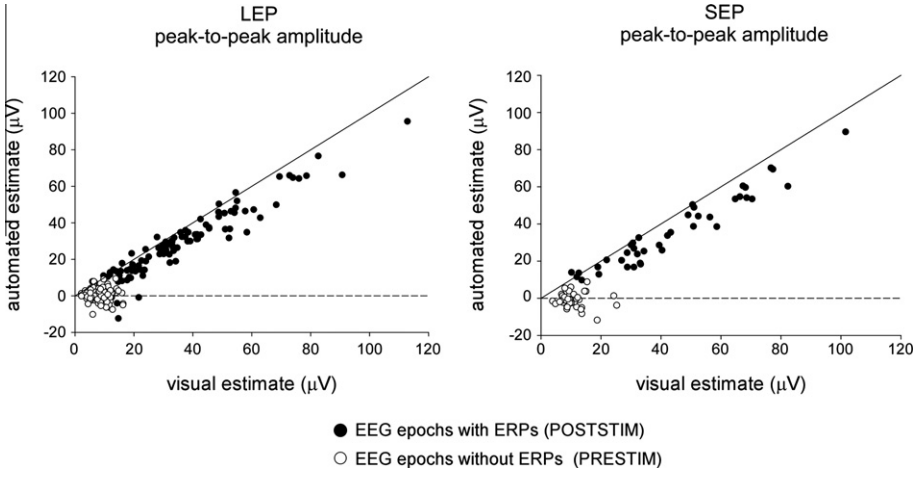

Fig. 2. Estimated peak-to-peak amplitude of the negative and positive waves of LEPs and SEPs identified in the average waveforms assumed to contain an ERP (POSTSTIM, shown in black), and in the average waveforms assumed not to contain an ERP (PRESTIM, shown in white), of healthy controls (*x-axis*: visual analysis, *y-axis*: single-trial automated analysis). The solid diagonal line represents the line of identity. Note the good absolute agreement between the two estimates, as illustrated by the proximity between the data and the line of identity.

Please cite this article in press as: Hatem SM et al. Automated single-trial assessment of laser-evoked potentials as an objective functional diagnostic tool for the nociceptive system. Clin Neurophysiol (2012), http://dx.doi.org/10.1016/j.clinph.2012.05.007

Table 1
Results of visual ERP analysis in patients and controls.

Visual identification	Patients $n = 37$	Controls $n = 21$
Right hand		
LEP N1 amplitude (μV)	−6 ± 5	−6 ± 6
N2-P2 amplitude (μV)	22 ± 12	29 ± 16
N1 latency (ms)	250 ± 55***	198 ± 21
N2 latency (ms)	293 ± 57**	253 ± 29
P2 latency (ms)	406 ± 73	397 ± 60
SEP N1-P2 amplitude (μV)	39 ± 17	45 ± 23
N1 latency (ms)	150 ± 42	137 ± 28
P2 latency (ms)	260 ± 63	277 ± 56
Left hand		
LEP N1 amplitude (μV)	−6 ± 4	−6 ± 4
N2-P2 amplitude (μV)	26 ± 15	30 ± 18
N1latency (ms)	223 ± 68	196 ± 20
N2 latency (ms)	269 ± 58	245 ± 22
P2 latency (ms)	389 ± 83	391 ± 67
SEP N1-P2 amplitude (μV)	45 ± 20	45 ± 24
N1 latency (ms)	144 ± 27	142 ± 30
P2 latency (ms)	263 ± 60	283 ± 51
Right shoulder		
LEP N1 amplitude (μV)	−7 ± 5	−7 ± 4
N2-P2 amplitude (μV)	27 ± 18	35 ± 26
N1 latency (ms)	220 ± 45***	178 ± 30
N2 latency (ms)	250 ± 56	229 ± 35
P2 latency (ms)	367 ± 74	372 ± 61
Left shoulder		
LEP N1 amplitude (μV)	−6 ± 3	−5 ± 4
N2-P2 amplitude (μV)	26 ± 14	35 ± 23
N1 latency (ms)	225 ± 54***	177 ± 28
N2 latency (ms)	251 ± 55	231 ± 29
P2 latency (ms)	373 ± 100	381 ± 73
Left face		
LEP N1 amplitude (μV)	−10 ± 11	−5 ± 4
N2-P2 amplitude (μV)	38 ± 16	38 ± 17
N1 latency (ms)	161 ± 36	144 ± 13
N2 latency (ms)	212 ± 38	203 ± 27
P2 latency (ms)	359 ± 77	375 ± 60

Univariate ANOVA (patients vs. controls).
** $p < 0.001$.
*** $p < 0.001$.

Table 2
Number of ERP average waveforms undetectable with the visual inspection.

	Number of waveforms recorded	Number of waveforms without a visually detectable ERP
Right hand		
LEPs	58	14 (24%)
SEPs	48	0 (0%)
Left hand		
LEPs	58	12 (21%)
SEPs	54	0 (0%)
Right shoulder		
LEPs	58	11 (19%)
Left shoulder		
LEPs	58	12 (21%)
Left face		
LEPs	58	(0%)

amplitudes were not significantly different from zero (LEP-N1: 0.2 ± 2 μV, $p = 0.060$; LEP-N2: −0.2 ± 3 μV, $p = 0.121$; LEP-P2: 0.2 ± 2 μV, $p = 0.060$) (see also Fig. 2).

Average post-stimulus waveforms categorized as containing or lacking an ERP using the two different ERP identification methods are shown in Fig. 4.

Table 3
Results of automated ERP analysis in patients and controls.

Automated identification	Patients $n = 37$	Controls $n = 21$
Right hand		
LEP N1 amplitude (μV)	−4 ± 6*	−8 ± 5
N2-P2 amplitude (μV)	14 ± 13*	23 ± 18
N1 latency (ms)	204 ± 32	200 ± 24
N2 latency (ms)	254 ± 45	245 ± 23
P2 latency (ms)	348 ± 92	336 ± 49
SEP N1-P2 amplitude (μV)	37 ± 21	36 ± 18
N1 latency (ms)	152 ± 41	140 ± 25
P2 latency (ms)	254 ± 59	276 ± 45
Left hand		
LEP N1 amplitude (μV)	−4 ± 6*	−8 ± 5
N2-P2 amplitude (μV)	16 ± 16*	27 ± 17
N1 latency (ms)	190 ± 30	181 ± 21
N2 latency (ms)	250 ± 37	250 ± 47
P2 latency (ms)	360 ± 56	367 ± 75
SEP N1-P2 amplitude (μV)	38 ± 17	36 ± 21
N1 latency (ms)	145 ± 31	147 ± 31
P2 latency (ms)	253 ± 61	277 ± 46
Right shoulder		
LEP N1 amplitude (μV)	−3 ± 5*	−6 ± 5
N2-P2 amplitude (μV)	18 ± 20*	29 ± 26
N1 latency (ms)	186 ± 39	178 ± 22
N2 latency (ms)	241 ± 52	233 ± 50
P2 latency (ms)	358 ± 87	352 ± 50
Left shoulder		
LEP N1 amplitude (μV)	−3 ± 4**	−7 ± 4
N2-P2 amplitude (μV)	14 ± 15*	26 ± 19
N1 latency (ms)	159 ± 34	156 ± 27
N2 latency (ms)	229 ± 33	237 ± 33
P2 latency (ms)	318 ± 90	335 ± 58
Left face		
LEP N1 amplitude (μV)	−5 ± 5	−5 ± 7
N2-P2 amplitude (μV)	33 ± 17	28 ± 18
N1 latency (ms)	156 ± 27	153 ± 21
N2 latency (ms)	204 ± 32	205 ± 32
P2 latency (ms)	312 ± 65	326 ± 64

Univariate ANOVA (patients vs. controls).
* $p < 0.050$.
** $p < 0.001$.

4. Discussion

The present study shows that the amplitudes and latencies of both normal and abnormal LEP and SEP peaks can be identified reliably using a novel automated approach based on wavelet denoising and single-trial ERP estimation with multiple linear regression in a clinical setting. Indeed, the sensitivity and specificity of the automated approach at detecting the presence vs. the absence of LEPs and SEPs was similar to the sensitivity and specificity of the more conventional approach based on the visual inspection of average ERP waveforms.

As mentioned in the Introduction, in the context of clinical studies, the quantification of ERP latency and amplitude by visual inspection becomes problematic when the elicited responses are altered beyond recognition. Indeed, discarding those ERP waveforms when performing group-level comparisons of peak amplitudes will inevitably lead to an underestimation of the observed differences. For this reason, several studies assign an arbitrary zero value to the amplitude of ERP waveforms that are visually unrecognized (e.g. Hatem et al., 2010; Quante et al., 2007; Rage et al., 2010). Inevitably, this will lead to an overestimation of observed differences. Furthermore, it is impossible to include those unrecognized ERP waveforms when comparing peak latencies. Finally, simply reporting the number of subjects in which no ERP can be visually identified is descriptive, and this qualitative categorization

Please cite this article in press as: Hatem SM et al. Automated single-trial assessment of laser-evoked potentials as an objective functional diagnostic tool for the nociceptive system. Clin Neurophysiol (2012), http://dx.doi.org/10.1016/j.clinph.2012.05.007

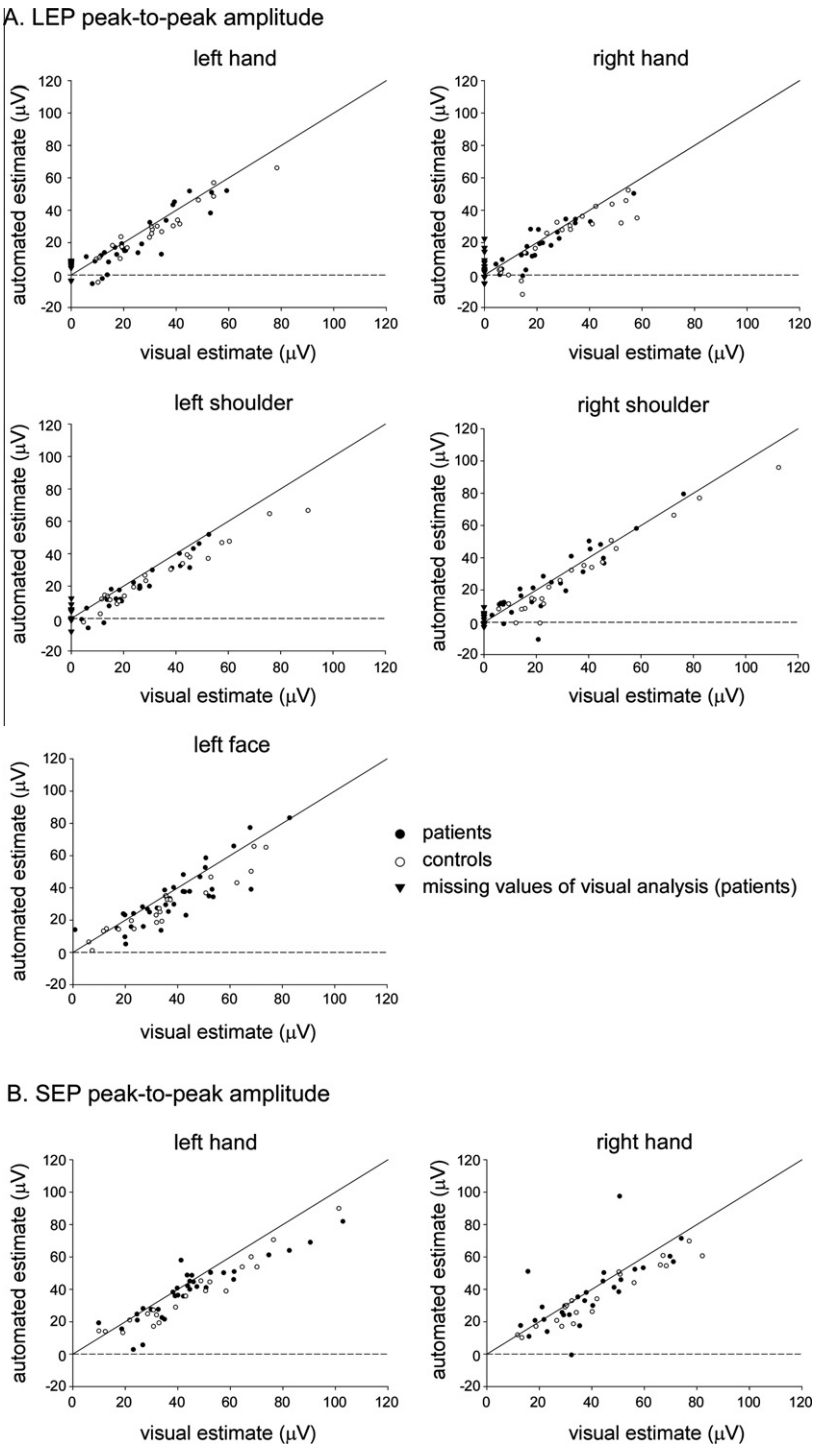

Fig. 3. Comparison of visual vs. automated estimates of the peak-to-peak amplitude of LEPs and SEPs in patients (black) and healthy controls (white). Note the good absolute agreement between the two estimates, as illustrated by the proximity between the data and the reference line of identity (solid line). Values where the observer could not identify any ERP (i.e. missing values) are represented as triangles on the *y-axis*.

may be subject to important observer-dependent biases. For this reason, the unbiased solution provided by the automated approach is of particular interest for clinical research aiming, for example, at comparing groups of patients, or assessing the effect of a given treatment.

The automated approach used in the present study assigns a latency and amplitude value to the ERP peaks of *each* single-trial waveform. Because estimation of these ERP peaks is based on the multiple linear regression of a basis set that can be fitted both negatively and positively, in the absence of an ERP, the average estimated amplitude using this automated approach will tend towards zero, thus avoiding any bias. However, because the approach yields an estimate of the amplitude and latency of ERP peaks even in waveforms where no ERP can be identified by visual inspection, missing values are avoided and the statistical power of group comparisons is increased. This effect was observed clearly in the present study where approximately 20% of the LEPs recorded from pathological stimulation sites in patients were considered as

Please cite this article in press as: Hatem SM et al. Automated single-trial assessment of laser-evoked potentials as an objective functional diagnostic tool for the nociceptive system. Clin Neurophysiol (2012), http://dx.doi.org/10.1016/j.clinph.2012.05.007

Table 4
Comparison of the visual and the automated identification of LEPs and SEPs in all subjects ($n = 58$).

Visual vs. automated identification			
	Visual	Automated	ICC single measure
Right hand			
LEP N1 amplitude (μV)	−6 ± 5	−5 ± 6	0.54***
N2-P2 amplitude (μV)	25 ± 14***	17 ± 15	0.83***
N1 latency (ms)	230 ± 51**	203 ± 29	0.09
N2 latency (ms)	274 ± 50**	251 ± 38	0.41**
P2 latency (ms)	402 ± 66***	344 ± 79	0.14
SEP N1-P2 amplitude (μV)	42 ± 20**	36 ± 19	0.74***
N1 latency (ms)	145 ± 38	147 ± 35	0.22
P2 latency (ms)	267 ± 60	263 ± 54	0.69***
Left hand			
LEP N1 amplitude (μV)	−6 ± 4	−6 ± 6	0.40**
N2-P2 amplitude (μV)	28 ± 17**	20 ± 17	0.88***
N1 latency (ms)	213 ± 56**	187 ± 27	−0.00
N2 latency (ms)	258 ± 46	250 ± 40	0.28*
P2 latency (ms)	390 ± 75**	362 ± 63	0.61***
SEP N1-P2 amplitude (μV)	45 ± 21***	38 ± 19	0.85***
N1 latency (ms)	143 ± 28	145 ± 31	0.50***
P2 latency (ms)	271 ± 57	262 ± 57	0.76***
Right shoulder			
LEP N1 amplitude (μV)	−7 ± 5**	−5 ± 5	0.49***
N2-P2 amplitude (μV)	30 ± 22**	22 ± 23	0.92***
N1 latency (ms)	204 ± 45**	183 ± 34	0.24*
N2 latency (ms)	240 ± 48	238 ± 51	0.30*
P2 latency (ms)	369 ± 67	356 ± 75	0.40**
Left shoulder			
LEP N1 amplitude (μV)	−5 ± 4*	−4 ± 5	0.46***
N2-P2 amplitude (μV)	30 ± 19***	19 ± 17	0.88***
N1 latency (ms)	207 ± 51***	158 ± 31	−0.13
N2 latency (ms)	241 ± 45	231 ± 33	0.30*
P2 latency (ms)	385 ± 67***	324 ± 80	0.30**
Left face			
LEP N1 amplitude (μV)	−8 ± 10*	−5 ± 5	0.14
N2-P2 amplitude (μV)	38 ± 17***	32 ± 17	0.81***
N1 latency (ms)	155 ± 31	155 ± 25	0.04
N2 latency (ms)	209 ± 34	204 ± 32	0.62***
P2 latency (ms)	365 ± 71***	317 ± 64	0.32***

Two-way mixed intra-class correlation coefficients with absolute agreement measures assessed the absolute agreement between measures (visual vs. automated). Paired *t*-tests (visual vs. automated).
* $p < 0.050$.
** $p < 0.010$.
*** $p < 0.001$.

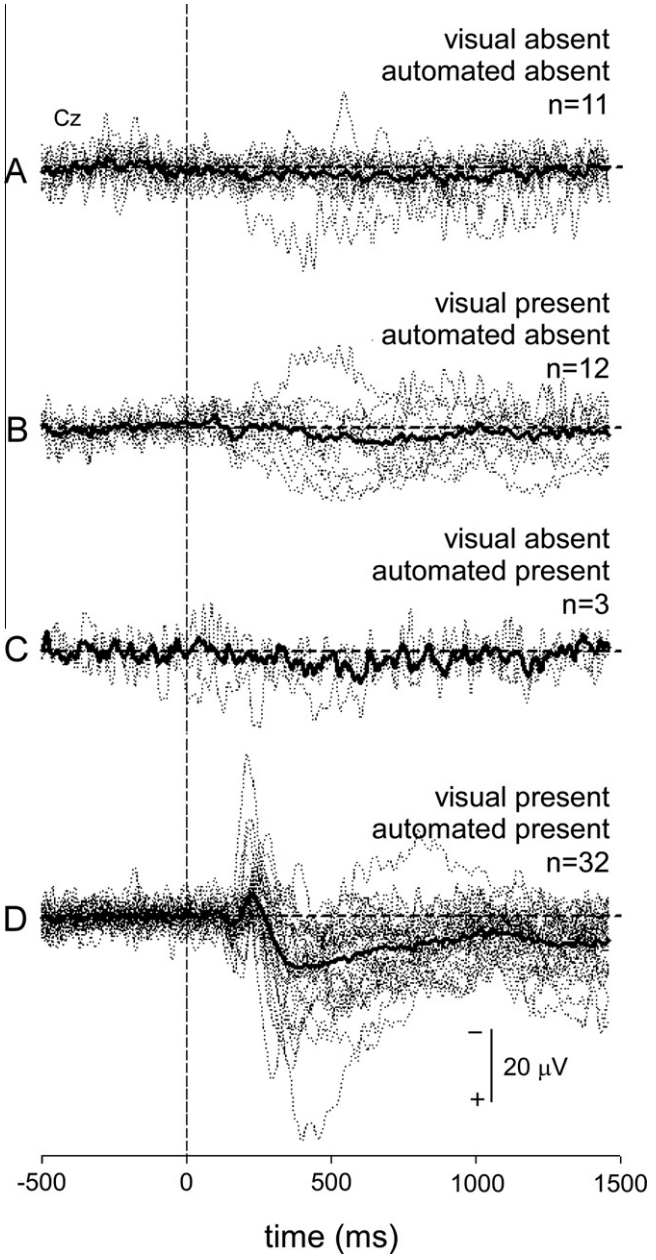

Fig. 4. Grand average (bold) and individual average (dotted) waveforms of LEPs recorded at electrode Cz vs. A1A2 during stimulation of the right hand ($n = 58$). In each average waveform, the ERP was categorized as absent or present based on either the automated analysis or the visual analysis. In the automated analysis, the presence vs. absence of LEPs was defined based on the optimal cutoff to discriminate between PRESTIM and POSTSTIM epochs in healthy controls (see Methods). In the visual analysis, presence vs. absence of LEPs was based on the decision of the observer. Based on this classification, LEP waveforms were categorized into the following four categories: (A) LEPs considered as absent with both methods ($n = 11$), (B) LEPs considered as absent with the automated method but present with the visual method ($n = 12$), (C) LEPs considered as present with the automated method but absent with the visual method ($n = 3$), and (D) LEPs considered as present with both methods ($n = 32$).

absent with the visual approach. The lack of significant differences between the ERPs of patients and controls estimated using the visual approach was thus clearly due to the important number of missing values in the patient group.

Even among experienced observers relying on clearly defined criteria to identify ERP peaks, a certain degree of divergence may exist in recognizing these peaks. In the present study, the overall inter-rater agreement of the measures of the amplitude and latency of LEP and SEP peaks performed by the two independent observers was good. Nonetheless, estimation of the laser-evoked P2 peak was significantly different between the two observers, probably because of the ambiguity between the LEP-P2 peak and the occasional presence of an additional later positive peak occurring in some subjects, thought to reflect an involuntary attentional shift towards the stimulus (Legrain et al., 2005; Siedenberg and Treede, 1996). This observation highlights the inherent subjectivity of ERP estimates based on visual inspection.

We found a strong agreement between the ERP estimates of amplitude and latency obtained using the visual approach and the automated approach. However, amplitude estimates obtained using the automated approach were slightly but significantly smaller than the amplitude estimates obtained using the visual approach. Furthermore, latency estimates obtained using the automated approach were slightly but significantly shorter as compared to the latency estimates obtained using the visual approach. These differences are likely to be explained by the fact that, in the visual approach, waveforms where no ERP could be identified were not included in the estimate of ERP amplitude and that automated estimates were based on a basis set constructed using the grand-average of all subjects. On the other hand,

Please cite this article in press as: Hatem SM et al. Automated single-trial assessment of laser-evoked potentials as an objective functional diagnostic tool for the nociceptive system. Clin Neurophysiol (2012), http://dx.doi.org/10.1016/j.clinph.2012.05.007

a single-subject approach in which a basis set would be constructed for each single subject, as used in previous studies (Hu et al., 2010; Luck, 2005), could not be applied as a template in possibly pathological conditions. Small mismatches between the visual and the automated approach could also be explained by the fact that visual inspection (1) could have categorized some average waveforms as containing an ERP albeit of very small amplitude based, for example, on the scalp topography of visualized peaks and (2) could have categorized some average waveforms as not containing an ERP because the presence of an important jitter across trials distorted the average ERP beyond recognition (Mouraux and Iannetti, 2008).

In summary, we show that a recently developed automated approach to measure the amplitude and latency of ERP peaks based on wavelet denoising and multiple linear regression can be used to efficiently and reliably estimate the LEP and SEP peaks recorded in patients presenting with a dysfunction of the nociceptive system. The sensitivity and specificity of the approach was similar to the more conventional method based on visual inspection. This does not mean that the visual inspection of ERPs should be abandoned. Indeed, it is highly likely that the trained eye of the expert integrates important features of the waveforms that are not taken into consideration by the automated analysis and, therefore, that visual inspection allows a richer and more efficient interpretation of ERPs. Instead, it indicates that, because the automated approach is efficient and, most importantly, entirely observer-independent, it could constitute a very useful tool for clinical research aiming, for example, at comparing groups of patients, or assessing the effect of a given treatment.

Acknowledgments

S.M. Hatem received a research fellow funding by the F.R.S. – FNRS (Belgium). G.D. Iannetti is University Research Fellow of the Royal Society (United Kingdom). This work was supported by INSERM (U-987). A. Mouraux received support from a Marie Curie European Reintegration Grant, as well as from the IASP 2010 Early Career Research Grant. We gratefully thank Ms. Michèle Gautron for technical and logistic assistance. There are no conflicts of interest.

References

Bromm B, Treede RD. Laser-evoked cerebral potentials in the assessment of cutaneous pain sensitivity in normal subjects and patients. Rev Neurol (Paris) 1991;147:625–43.

Carmon A, Mor J, Goldberg J. Evoked cerebral responses to noxious thermal stimuli in humans. Exp Brain Res 1976;25:103–7.

Casanova-Molla J, Grau-Junyent JM, Morales M, Valls-Sole J. On the relationship between nociceptive evoked potentials and intraepidermal nerve fiber density in painful sensory polyneuropathies. Pain 2011;152:410–8.

Casey KL, Beydoun A, Boivie J, Sjolund B, Holmgren H, Leijon G, et al. Laser-evoked cerebral potentials and sensory function in patients with central pain. Pain 1996;64:485–91.

Cruccu G, Aminoff MJ, Curio G, Guerit JM, Kakigi R, Mauguiere F, et al. Recommendations for the clinical use of somatosensory-evoked potentials. Clin Neurophysiol 2008;119:1705–19.

Cruccu G, Sommer C, Anand P, Attal N, Baron R, Garcia-Larrea L, et al. EFNS guidelines on neuropathic pain assessment: revised 2009. Eur J Neurol 2010;17:1010–8.

Garcia-Larrea L, Convers P, Magnin M, Andre-Obadia N, Peyron R, Laurent B, et al. Laser-evoked potential abnormalities in central pain patients: the influence of spontaneous and provoked pain. Brain 2002;125:2766–81.

Garcia-Larrea L, Frot M, Valeriani M. Brain generators of laser-evoked potentials: from dipoles to functional significance. Neurophysiol Clin 2003;33:279–92.

Haanpaa M. Are neuropathic pain screening tools useful for patients with spinal cord injury? Pain 2011;152:715–6.

Haanpaa M, Attal N, Backonja M, Baron R, Bennett M, Bouhassira D, et al. NeuPSIG guidelines on neuropathic pain assessment. Pain 2011;152:14–27.

Hatem SM, Attal N, Ducreux D, Gautron M, Parker F, Plaghki L, et al. Assessment of spinal somatosensory systems with diffusion tensor imaging in syringomyelia. J Neurol Neurosurg Psychiatry 2009;80:1350–6.

Hatem SM, Attal N, Ducreux D, Gautron M, Parker F, Plaghki L, et al. Clinical, functional and structural determinants of central pain in syringomyelia. Brain 2010;133:3409–22.

Hatem SM, Plaghki L, Mouraux A. How response inhibition modulates nociceptive and non-nociceptive somatosensory brain-evoked potentials. Clin Neurophysiol 2007;118:1503–16.

Hu L, Mouraux A, Hu Y, Iannetti GD. A novel approach for enhancing the signal-to-noise ratio and detecting automatically event-related potentials (ERPs) in single trials. Neuroimage 2010;50:99–111.

Hu L, Zhang ZG, Hung YS, Luk KD, Iannetti GD, Hu Y. Single-trial detection of somatosensory evoked potentials by probabilistic independent component analysis and wavelet filtering. Clin Neurophysiol 2011;122:1429–39.

Jung TP, Makeig S, Humphries C, Lee TW, McKeown MJ, Iragui V, et al. Removing electroencephalographic artifacts by blind source separation. Psychophysiology 2000;37:163–78.

Kakigi R, Kuroda Y, Neshige R, Endo C, Shibasaki H. Physiological study of the spinothalamic tract conduction in multiple sclerosis. J Neurol Sci 1992;107:205–9.

Kakigi R, Shibasaki H, Kuroda Y, Neshige R, Endo C, Tabuchi K, et al. Pain-related somatosensory evoked potentials in syringomyelia. Brain 1991;114:1871–89.

Kramer AF. The interpretation of the component structure of event-related brain potentials: an analysis of expert judgments. Psychophysiology 1985;22:334–44.

Lawless JF. Statistical models and methods for lifetime data. 2nd ed. Hoboken: Wiley; 2003.

Legrain V, Bruyer R, Guerit JM, Plaghki L. Involuntary orientation of attention to unattended deviant nociceptive stimuli is modulated by concomitant visual task difficulty. Evidence from laser evoked potentials. Clin Neurophysiol 2005;116:2165–74.

Luck SJ. An introduction to the event-related potential technique. Cambridge: MIT Press; 2005.

Mayhew SD, Iannetti GD, Woolrich MW, Wise RG. Automated single-trial measurement of amplitude and latency of laser-evoked potentials (LEPs) using multiple linear regression. Clin Neurophysiol 2006;117:1331–44.

Moher D, Hopewell S, Schulz KF, Montori V, Gotzsche PC, Devereaux PJ, et al. CONSORT 2010 explanation and elaboration: updated guidelines for reporting parallel group randomised trials. BMJ 2010;340:c869.

Mouraux A, Guerit JM. Automated single-trial detection and quantification of evoked potentials, a potential tool for neuromonitoring? Clin Neurophysiol 2011;122:1280–1.

Mouraux A, Iannetti GD. Across-trial averaging of event-related EEG responses and beyond. Magn Reson Imaging 2008;26:1041–54.

Mouraux A, Plaghki L. Single-trial detection of human brain responses evoked by laser activation of Adelta-nociceptors using the wavelet transform of EEG epochs. Neurosci Lett 2004;361:241–4.

Orstavik K, Namer B, Schmidt R, Schmelz M, Hilliges M, Weidner C, et al. Abnormal function of C-fibers in patients with diabetic neuropathy. J Neurosci 2006;26:11287–94.

Plaghki L, Mouraux A. How do we selectively activate skin nociceptors with a high power infrared laser? Physiology and biophysics of laser stimulation. Neurophysiol Clin 2003;33:269–77.

Quante M, Hauck M, Gromoll M, Hille E, Lorenz J. Dermatomal laser-evoked potentials: a diagnostic approach to the dorsal root. Norm data in healthy volunteers and changes in patients with radiculopathy. Eur Spine J 2007;16:943–52.

QuianQuiroga R, Garcia H. Single-trial event-related potentials with wavelet denoising. Clin Neurophysiol 2003;114:376–90.

Rage M, Van Acker N, Facer P, Shenoy R, Knaapen MW, Timmers M, et al. The time course of CO(2) laser-evoked responses and of skin nerve fibre markers after topical capsaicin in human volunteers. Clin Neurophysiol 2010;121:1256–66.

Siedenberg R, Treede RD. Laser-evoked potentials: exogenous and endogenous components. Electroencephalogr Clin Neurophysiol 1996;100:240–9.

Spiegel J, Hansen C, Baumgartner U, Hopf HC, Treede RD. Sensitivity of laser-evoked potentials versus somatosensory evoked potentials in patients with multiple sclerosis. Clin Neurophysiol 2003;114:992–1002.

Treede RD, Lankers J, Frieling A, Zangemeister WH, Kunze K, Bromm B. Cerebral potentials evoked by painful, laser stimuli in patients with syringomyelia. Brain 1991;114:1595–607.

Treede RD, Lorenz J, Baumgartner U. Clinical usefulness of laser-evoked potentials. Neurophysiol Clin 2003;33:303–14.